CHEMISTRY OF MATERIALS
Communication

Chem. Mater. **2010,** *22,* 9–11 9
DOI:10.1021/cm9014783

Phase-Controlled Synthesis of Colloidal In_2O_3 Nanocrystals via Size-Structure Correlation

Shokouh S. Farvid, Neeshma Dave, and Pavle V. Radovanovic*

Department of Chemistry, University of Waterloo, 200 University Avenue West, Waterloo, Ontario N2L 3G1, Canada

Received May 29, 2009
Revised Manuscript Received November 20, 2009

Control and manipulation of crystal structures has important implications for the design and preparation of new solid-state materials. The ability to obtain metastable high-energy structures in a controlled way requires fundamental understanding of the phase transformation mechanisms.[1,2] The kinetics of phase transitions in nanocrystals (NCs) are generally less complex than those in bulk because of their large surface areas and a low number of crystal lattice defects.[2] As such, colloidal NCs offer a unique opportunity to control metastability and manipulate structural transformations in solutions.

Transparent conducting oxides (TCOs) have significant technological importance because of their unique optical and electrical properties. Among TCOs, In_2O_3 is one of the most widely applied because of its transparency ($E_g \approx 3.75$ eV), electrical conductivity (native n-type semiconductor), and high charge-carrier mobility.[3] Because of these characteristics, In_2O_3 has been employed in batteries, solar cells, electrodes, displays, and sensors.[4,5] The stable form of In_2O_3 has body-centered cubic bixbyite-type crystal structure (*bcc*-In_2O_3, $Ia\bar{3}$) in which In^{3+} cations reside in two characteristic sites, known as b- and d-sites (see Figure S1 in the Supporting Information). The metastable corundum-type In_2O_3[6] has rhombohedral structure (*rh*-In_2O_3, $R3\bar{c}$) consisting of hexagonal close-packed oxygen ions with In^{3+} cations filling up two-thirds of the octahedral sites (see Figure S2 in the Supporting Information). The stabilization of metastable corundum-type In_2O_3 has been achieved by conversion of *bcc*-In_2O_3 at high pressures and temperatures.[7,8] For doped In_2O_3, the stabilization of the rhombohedral phase has been associated with incorporation of smaller cations such as Fe^{3+} and Sn^{4+}.[9] Direct preparations of *rh*-In_2O_3 powders under ambient pressure involving calcination of $In(OH)_3$ or InOOH precursors have been reported.[10−12] The size-controlled *rh*-In_2O_3 nanocubes dispersible in organic solvents have been prepared from indium-isopropoxide in a multiple step synthesis based on dehydration of initially prepared InOOH nanoparticles.[13] Other syntheses of truly colloidal In_2O_3 NCs report only *bcc*-In_2O_3.[14−17] Although the stabilization of nanocrystalline *rh*-In_2O_3 has been related to solvents used for preparing the precursors[5,10,11] or the necessity of InOOH formation,[11,13] to the best of our knowledge the direct investigation of the In_2O_3 NC growth has not been reported. Here we report the study of the morphological and phase transformations of In_2O_3 NCs during their growth in solution, and show that *rh*-In_2O_3 is a transient structure in the formation of *bcc*-In_2O_3 NCs. We demonstrate a direct correlation between the nanocrystal size and structure, which allows for the stabilization of *rh*-In_2O_3 for NCs smaller than 5 nm under applied conditions. These results enable a direct and highly selective synthesis of colloidal In_2O_3 NCs having different phases.

The growth of colloidal In_2O_3 NCs was studied using a single-step procedure[14] which enables a convenient monitoring of the reaction products over time. In a typical synthesis a mixture of indium(III) acetylacetonate, $In(acac)_3$ (4 mmol, 98% STREM), and oleylamine (48 mmol, 70% Aldrich) was degassed and slowly heated in a 100 mL round-bottom flask to 250 °C under argon. The mixture was subsequently refluxed in the argon atmosphere. The aliquots were taken at different times during the reaction, and the products were precipitated and washed three times with ethanol.[18] The obtained

*Corresponding author e-mail: pavler@sciborg.uwaterloo.ca.

(1) Tolbert, S. H.; Alivisatos, A. P. *Annu. Rev. Phys. Chem.* **1995**, *46*, 595.
(2) Chen, C.-C.; Herhold, A. B.; Johnson, C. S.; Alivisatos, A. P. *Science* **1997**, *276*, 398.
(3) Hamberg, I.; Granqvist, C. G. *J. Appl. Phys.* **1986**, *60*, R123.
(4) Wang, D.; Zou, Z.; Ye, J. *Chem. Mater.* **2005**, *17*, 3255. Li, X.; Wanlass, M. W.; Gessert, T. A.; Emery, K. A.; Coutts, T. J. *Appl. Phys. Lett.* **1989**, *54*, 2674. Du, N.; Zhang, H.; Chen, J.; Sun, J.; Chen, B.; Yang, D. *J. Phys. Chem. B* **2008**, *112*, 14836.
(5) Chu, D.; Zeng, Y.-P.; Jiang, D.; Xu, J. *Nanotechnology* **2007**, *18*, 435605.
(6) Gurlo, A.; Kroll, P.; Riedel, R. *Chem. Eur. J.* **2008**, *14*, 3306.
(7) Shannon, R. D. *Solid State Commun.* **1966**, *4*, 629.
(8) Prewitt, C. T.; Shannon, R. D.; Rogers, D. B.; Sleight, A. W. *Inorg. Chem.* **1969**, *8*, 1985.
(9) Frank, G.; Olazcuaga, R.; Rabenau, A. *Inorg. Chem.* **1977**, *16*, 1251. Gurlo, A.; Ivanovskaya, M.; Barsan, N.; Weimar, U. *Inorg. Chem. Commun.* **2003**, *6*, 569. Chu, D.; Zeng, Y.-P.; Jiang, D.; Ren, Z. *Appl. Phys. Lett.* **2007**, *91*, 262503.
(10) Epifani, M.; Siciliano, P.; Gurlo, A.; Barsan, N.; Weimar, U. *J. Am. Chem. Soc.* **2004**, *126*, 4078.
(11) Yu, D.; Wang, D.; Qian, Y. *J. Solid State Chem.* **2004**, *177*, 1230.
(12) Chen, C.; Chen, D.; Jiao, X.; Wang, C. *Chem. Commun.* **2006**, 4632.
(13) Lee, C. H.; Kim, M.; Kim, T.; Kim, A.; Paek, J.; Lee, J. W.; Choi, S.-Y.; Kim, K.; Park, J.-B.; Lee, K. *J. Am. Chem. Soc.* **2006**, *128*, 9326.
(14) Farvid, S. S.; Ju, L.; Worden, M.; Radovanovic, P. V. *J. Phys. Chem. C* **2008**, *112*, 17755. Seo, W. S.; Jo, H. H.; Lee, K.; Park, J. T. *Adv. Mater.* **2003**, *15*, 795.
(15) Liu, Q.; Lu, W.; Ma, A.; Tang, J.; Lin, J.; Fang, J. *J. Am. Chem. Soc.* **2005**, *127*, 5276.
(16) Narayanaswamy, A.; Xu, H.; Pradhan, N.; Kim, M.; Peng, X. *J. Am. Chem. Soc.* **2006**, *128*, 10310.
(17) Franzman, M. A.; Perez, V.; Brutchey, R. L. *J. Phys. Chem. C* **2009**, *113*, 630.
(18) In as-synthesized samples the surface terminations induce some NC aggregation. This can be improved by subsequent coordination of NCs with a protective ligand such as TOPO. The centrifuged NCs were added to molten TOPO, stirred at 150 °C and precipitated with ethanol. This procedure was repeated 3 times, and the obtained NCs were suspended in organic solvents.

Published on Web 12/08/2009

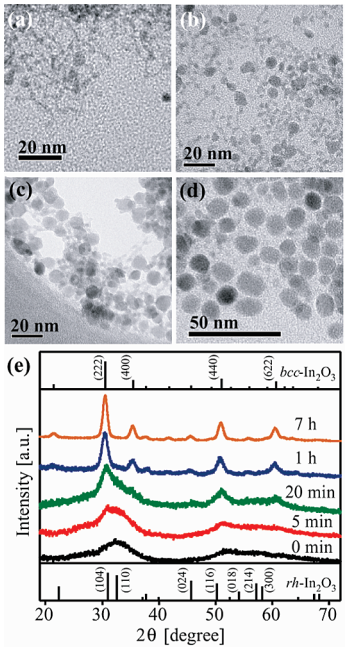

Figure 1. (a−d) TEM images of nanocrystalline In_2O_3 during the synthesis at 250 °C: (a) 0, (b) 10, (c) 30, and (d) 60 min upon reaching the reaction temperature. (e) XRD patterns of In_2O_3 NCs at different times during the synthesis at 250 °C. Vertical lines at the top and bottom represent the patterns of bulk *bcc*-In_2O_3 (JCPDS 06−0416) and *rh*-In_2O_3 (JCPDS 21−0406), respectively, with major reflections assigned.

samples were then suspended in toluene, hexane, or other organic solvents. For the selective synthesis of *bcc*-In_2O_3 and *rh*-In_2O_3 NCs, the reaction was continuously run at different temperatures and for different amounts of time (vide infra) and then slowly cooled to room temperature, yielding a viscous suspension of NCs. These NCs were precipitated and washed with ethanol, functionalized with trioctylphosphine oxide (TOPO), and suspended in organic solvents.[18]

Transmission electron microscopy (TEM) images of the products obtained at different times during the synthesis are shown in Figure 1. Immediately upon reaching the final reaction temperature the samples have a network-like structure with a few sub-5 nm particles imbedded in the network (Figure 1a). After 10 min, the number of nanoparticles increases with respect to the nanostructured network, and they become larger and faceted (Figure 1b). This process continues over time (30 min, Figure 1c), and after 1 h the network completely disappears, leaving behind only nanoparticles that are much more uniform in size (Figure 1d). XRD patterns of several representative samples collected at different times during the synthesis are shown in Figure 1e. All samples are crystalline, although broadening of the XRD peaks decreases for products obtained at longer reaction times because of an increase in the size of the crystalline domains. Surprisingly, a change in the crystal structure was observed during the reaction. The XRD pattern of the initially formed thin-walled networks is in good agreement with that of bulk *rh*-In_2O_3. As the reaction proceeds, the peaks corresponding to *bcc*-In_2O_3 become apparent. These peaks are significantly narrower than the peaks corresponding to *rh*-In_2O_3, indicating that the change in NC structure from rhombohedral to cubic accompanies an increase in NC size. These observations strongly suggest that metastable *rh*-In_2O_3 is an intermediate structure in the formation of *bcc*-In_2O_3 during NC growth. For small NC sizes, the phase transformations are strongly influenced by surfaces, and the surface free-energy contribution can reverse the relative stability of different polymorphs.[19,20] This phenomenon has been associated with higher concentration of unsatisfied charges on stable polymorph surfaces, which raise their free energies relative to those of a metastable phase.[20] Furthermore, a higher local electron density on surfaces with respect to that in bulk is responsible for an increase in surface interatomic distances in order to partially compensate for the difference in charge density. Such a change in surface bonding causes a negative (compressive) surface stress.[21] This process would also favor the stabilization of *rh*-In_2O_3, which has a slightly higher density (ca. 2.6%) than *bcc*-In_2O_3.[8]

To verify the role of other intermediates in this single-step procedure, we performed the reaction at lower temperatures. The formation of nanocrystalline InOOH at temperatures as low as 150 °C was observed in XRD patterns (see Figure S3 in the Supporting Information). The formation of InOOH has been signified as the key step in obtaining *rh*-In_2O_3 at ambient pressure.[11−13] The presence of $In(OH)_3$[11] or the absence of added water,[13] on the other hand, were suggested to prevent *rh*-In_2O_3 stabilization, although $In(OH)_3$ has been identified by other authors[5,10] as a precursor from which both *bcc*-In_2O_3 and *rh*-In_2O_3 can form. Corundum-type In_2O_3 has not been observed or reported when $In(acac)_3$ was used as a precursor.[14,17] These discrepancies indicate a sensitivity of the obtained product to the reaction conditions and point out the importance of systematic studies of the In_2O_3 NC formation in solution. Here we used $In(acac)_3$ precursor and showed that both *rh*- and *bcc*-In_2O_3 are derived from InOOH, which is formed by dehydration of $In(OH)_3$. Water-free synthesis in nonbasic organic solvents did not yield any NCs indicating that controlled presence of small amounts H_2O in oleylamine is needed for $In(OH)_3$ and InOOH formation by hydrolysis. Control experiments using $In(NO_3)_3$ precursor showed the same trend suggesting that In_2O_3 NCs are generally formed by hydrolysis mechanisms in solution phase preparations involving In^{3+} salt precursors.[16]

Understanding the growth mechanism and the structural transformation should allow for the rational and controlled preparation of colloidal In_2O_3 NCs having specific sizes and structures by simply adjusting the reaction conditions, including temperature, precursors, solvents, coordinating ligands, and reaction time. We hypothesized that a rapid NC growth would lead to fast transformation of *rh*-In_2O_3, resulting in *bcc*-In_2O_3 NCs.

(19) McHale, J. M.; Auroux, A.; Perrotta, A. J.; Navrotsky, A. *Science* **1997**, *277*, 788.
(20) Zhang, H.; Banfield, J. F. *J. Mater. Chem* **1998**, *8*, 2073.
(21) Blakely, J. M. *Introduction to the Properties of Crystal Surfaces*, 1st ed.; Pergamon Press: Oxford, U.K., 1973; Vol. *12*.

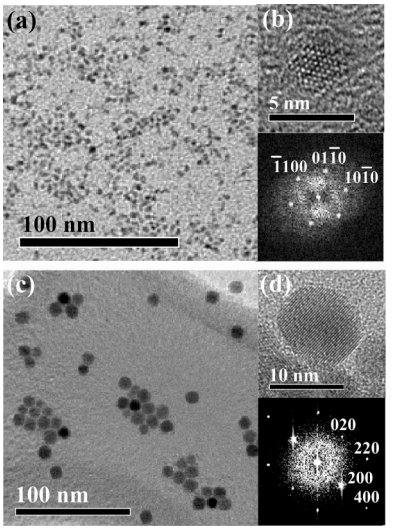

Figure 2. (a, c) Overview TEM images of (a) *rh*-In_2O_3 NCs synthesized at 200 °C for 30 h, and (c) *bcc*-In_2O_3 NCs synthesized at 250 °C for 30 h. (b, d) Lattice-resolved TEM (top) and the corresponding FFT images (bottom) of (b) a single *rh*-In_2O_3, and (d) *bcc*-In_2O_3 NC.

A decrease in the growth rate would lead to formation of small NCs and the stabilization of *rh*-In_2O_3. Starting from this premise, we optimized the reaction temperatures and times to selectively obtain high purity *rh*-In_2O_3 and *bcc*-In_2O_3 NCs while keeping all other parameters the same. Figure 2a shows a TEM image of In_2O_3 NCs synthesized at 200 °C for 30 h. Well-defined NCs having an average size of ca. 3.5 nm and the corundum-type crystal structure (XRD in Figure 3a, bottom) are observed. High-resolution TEM and the corresponding fast Fourier transform (FFT) images (Figure 2b) confirm the crystal structure at the single NC level. Figure 2c,d shows TEM images of a sample synthesized at 250 °C for 30 h. The resulting NCs have an average size of ca. 9.5 nm and cubic bixbyite-type structure, evidenced by TEM/FFT images (Figure 2c,d) and the XRD pattern (Figure 3a, top). The purity of the obtained NC phases was confirmed by Raman spectroscopy. The spectrum of NCs from Figure 2a shows the dominant peak characteristic for *rh*-In_2O_3[22] (Figure 3b, bottom), with no evidence of the presence of *bcc*-In_2O_3. Raman spectrum of NCs from Figure 2c is in excellent agreement with that documented for the bixbyite phase,[22] suggesting purely *bcc*-In_2O_3 NCs (Figure 3b, top). The transformation of *rh*- to *bcc*-In_2O_3 NCs is determined by the NC growth kinetics. At 250 °C NCs grow rapidly and the transient *rh*-In_2O_3 could be isolated only after short times (Figure 1a,b). Further increase in the reaction temperature yielded only *bcc*-In_2O_3 NCs (see Figure S4 in the Supporting Information). Similarly, the addition of water, a reactant in hydrolysis, to the reaction mixture at 200 °C, which otherwise yielded only *rh*-In_2O_3 NCs, resulted in an increase in the NC growth rate and the formation of *bcc*-In_2O_3 NCs (see Figure S5 in the Supporting Information). In the methodology used in this work, the largest *rh*-In_2O_3 NCs that could be stabilized are ca. 5 nm, which can be compared to 6.5 GPa at 1250 °C needed to convert bulk *bcc*-In_2O_3 to *rh*-In_2O_3.[8] A decrease in the growth rate and an increase in the NC surface stabilization at higher temperatures by manipulating other parameters[23] may result in larger *rh*-In_2O_3 NCs.

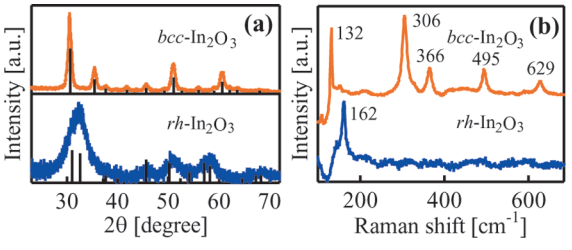

Figure 3. (a) XRD patterns of *rh*-In_2O_3 NCs synthesized at 200 °C for 30 h (bottom), and *bcc*-In_2O_3 NCs synthesized at 250 °C for 30 h (top). Black lines represent the XRD patterns of the corresponding bulk phases. (b) Raman spectra of *rh*-In_2O_3 (bottom) and *bcc*-In_2O_3 NCs (top).

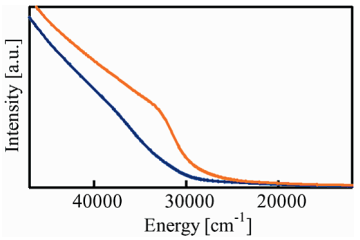

Figure 4. UV absorption spectra of 9.5 nm *bcc*-In_2O_3 (orange) and 3.5 nm *rh*-In_2O_3 NCs (blue), showing the band gap transitions.

The optical absorption spectra of these *bcc*- and *rh*-In_2O_3 NCs are shown in Figure 4. Strong transitions with the shoulderlike maxima at ca. 32500 and 37500 cm^{-1} are observed for *bcc*-In_2O_3 and *rh*-In_2O_3 NCs, respectively. These transitions are assigned to the band gap absorptions. The blue shift in the *rh*-In_2O_3 NC band gap transition is suggestive of a strong quantum confinement.

Structural transformations in NCs have previously been achieved at high pressures or temperatures, and studied as a function of these parameters.[1,2] In this communication, we demonstrated that NC phase transformations can be achieved in solution by controlling the NC growth rate and sizes. Understanding the formation and phase transformations of colloidal NCs allows for simultaneous tuning of their crystal and electronic structures. We believe that these findings can be applied to other materials that exhibit metastability, allowing for an expansion of the available NC building blocks through simple chemical approaches.

Acknowledgment. This work was supported by NSERC-Discovery grant and Canada Research Chairs Program.

Supporting Information Available: Figures S1−S5 (PDF). This material is available free of charge via the Internet at http://pubs.acs.org.

(22) Wang, C. Y.; Dai, Y.; Pezoldt, J.; Lu, B.; Kups, T.; Cimalla, V.; Ambacher, O. *Cryst. Growth Des.* **2008**, *8*, 1257.

(23) Farvid, S. S.; Dave, N.; Wang, T.; Radovanovic, P. V. *J. Phys. Chem. C* **2009**, *113*, 15928.